

# CONTINUOUS-FLOW DEPULPING MACHINE FOR *TRECVLIA AFRICANA*

---

S. O. ENIBE, C. P. ASIEGBU AND H. O. NJOKU

(Received 11, January 2010; Revision Accepted 14, March 2010)

## ABSTRACT

A continuous flow machine for the depulping of partially fermented fruit of *Treculia Africana* is presented. The machine is designed to improve upon an existing batch depulper, and consists of four main units, namely the hopper/depulping chamber, the connector-pipe, the separation chamber and power system. The machine operation involves the introduction of fermented breadfruit into the hopper from where it falls under gravity into the de-pulping chamber for further processing. The combination of crank and separation chamber is idealized as a six-member crank-rocker mechanism. Detailed kinematic and dynamic analysis of the idealized system is undertaken using an existing computer programme, SIXBAR. In this way, appropriate dimensions of each element are determined. A laboratory scale model of the machine is constructed and tested. Preliminary results indicate that 69–93% of the seeds could be effectively depulped. Further work is continuing to improve on the system performance and its acceptability by the stakeholders.

**KEYWORDS:** African breadfruit, SIXBAR programme, depulping machine.

## 1. INTRODUCTION

*Treculia Africana*, commonly called *African Breadfruit*, is a tree crop common in Southern Nigeria and in some parts of Ghana. It belongs to the taxonomic family *Murceae*, genus *Treculia*. A typical view of the tree, fruit attachment and leaf structure are shown in parts (a), (b) and (c) of figure 1.

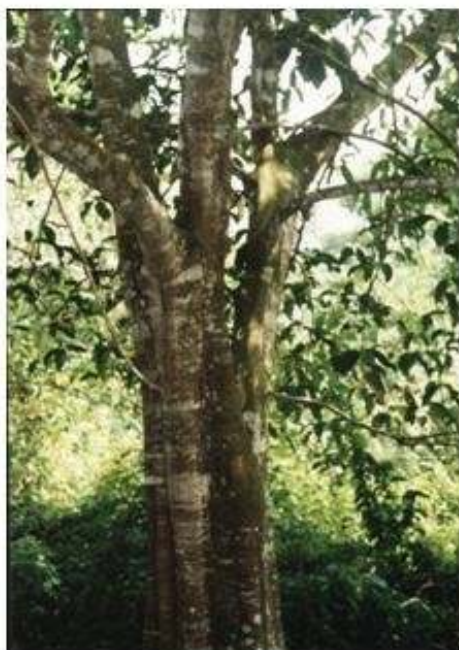
The crop is a rich source of high quality vegetable protein, oils and carbohydrates (Omobuwajo *et al*, 1999a, 1999b; Enibe, 2001).

Its potential for widespread application in the production of weaning foods, beverages and animal feeds has also been acknowledged (Ezeokonkwo, 2003).

The traditional methods of processing *Treculia Africana* consumes considerable amounts of water, human energy and time. In order to remove this drudgery, Enibe (2001) developed a batch depulping machine. While this machine had many advantages over the traditional methods, its operation is rather noisy and consumes considerable amounts of water.

---

S. O. Enibe, Department of Mechanical Engineering, University of Nigeria, Nsukka, Nigeria  
C. P. Asiegbu, Department of Mechanical Engineering, University of Nigeria, Nsukka, Nigeria  
H. O. Njoku, Department of Mechanical Engineering, University of Nigeria, Nsukka, Nigeria



**(a)** *T. africana* showing characteristic fluting of trunk



**(b)** Fruit attachment to the stem in *T. africana*



**(c)** Typical simple leaf of *T. africana*

**Figure 1:** Treculia africana tree showing fruit attachment and leaf structure  
Source: Mbah (2005)

To overcome these remaining problems, as well as increase the processing capacity, the development of a continuous flow machine has been undertaken.

**2. DESIGN**

The present machine was designed to achieve the following objectives:

1. **Low Cost:** The machine was conceived to be cheap to fabricate, operate and maintain, and this was achieved by the use of readily available materials in constructing the machine.
2. **Ease of Fabrication, Operation, Assembly and De-assembly for maintenance:** This was achieved by the extensive use of screw fasteners to hold different components together.
3. **Durability:** The various components were designed to be durable in order to eliminate frequent breakdown of the machine.

4. **Minimal water consumption.**
5. **Minimal manual handling:** This was in order eliminate the messy nature of the traditional processing method, and this was achieved by the continuous flow process of operation.

As reported in Enibe (2001), the minor diameter of the seeds is of the order of 4.98mm. Further, it is desirable that upon complete decomposition of the fruit head, the sliminess of the pulp would have been eliminated, and decomposed pulp will not stick to the walls of the separation chamber. It was also assumed that the fruit to be processed has fermented for about 3–9 days before being introduced into the depulping machine.

**2.1 General Description**

Drawing from the experiences gained in our previous work, a continuous flow machine with the general appearance shown in figure 2 was conceived.

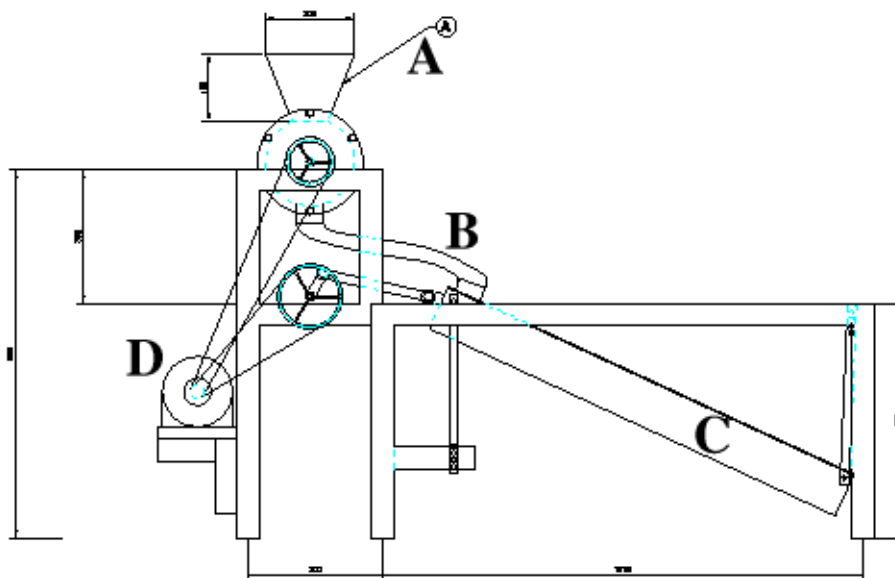


**Figure 2:** General view of the continuous flow depulping machine  
**A:** Hopper/depulping chamber; **B:** Connector; **C:** Separator; **D:** power transmission system

The machine consists essentially of four (4) main components, namely the hopper/depulping chamber, connector pipe, separator, and power system.

The decomposed mass is introduced into

the hopper from where it falls under gravity into the de-pulping chamber. The fruit is digested by the action of rotating spikes welded to flat bars, mounted on a hub. The digested slurry then flows through a flexible connector from the de-pulping

chamber into the separation chamber.

Inside the separation chamber, separation of the seeds from the pulp is achieved by the reciprocation of the tray and the force of falling water jets from the spray box. Due to the inclination of the tray, the seeds flow downward towards the separation chamber outlet, but their rate of descent is restricted and controlled by inclined baffles, so that the seeds are retained long enough in the tray to achieve complete separation.

The rotation of the separation chamber is achieved by the action of a crank to which it is connected, which is in turn connected to an electric motor by means of a V-belt. The electric motor also transmits rotary motion by means of

another V-belt to the de-pulping chamber shaft.

The washed out pulp is collected in a pit below the separation tray, and processed seeds collected at the exit of the separation tray. The whole structure is supported on a frame made of angle bars.

## 2.2 Hopper and Depulping Chamber

The hopper consists of the inverted frustum of a hollow cone. Based on considerations of overall machine dimensions, and seed angle of repose, the hopper was constructed with a total volume of 2.45 litres. Considering corrosion resistance and strength, gauge 20 galvanized steel is chosen for the construction. A development sketch of the hopper is shown in figure 3.

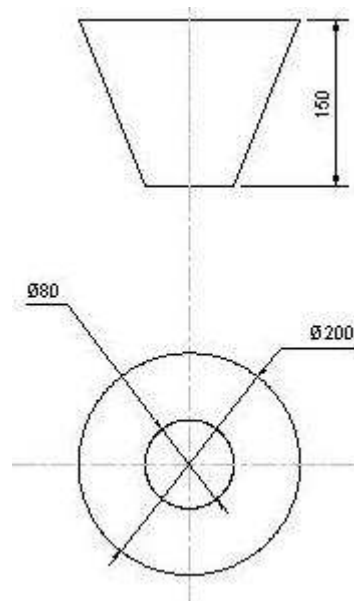


**Figure 3:** Development drawing of the hopper

The hopper is integrated with the depulping chamber which consists of a flanged cylinder for joining the face-plate with nuts and

bolts. The chamber housing has an inner diameter of 200mm and is 170mm long, as shown in figure 4.

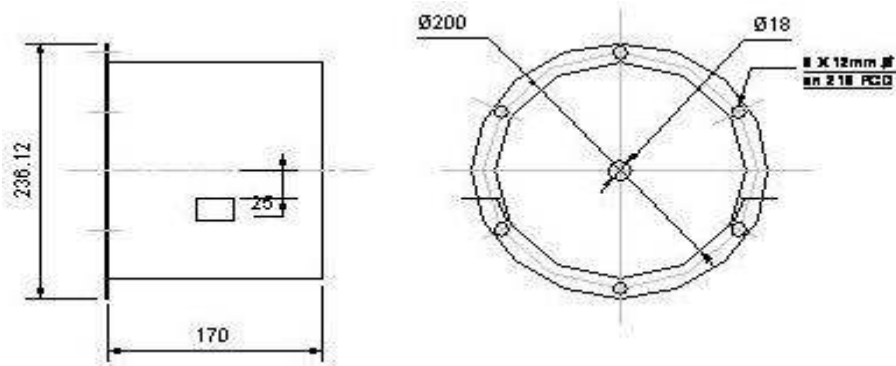


**Figure 4:** Depulping chamber housing

The cylinder is closed at the rear end with a plate having a 23mm diameter opening to allow passage of de-pulper shaft. The face-plate is dimensioned to fit and cover the front of the

chamber housing, as shown in figure 5. Galvanized steel is chosen for the chamber housing and face-plate to minimise corrosion.

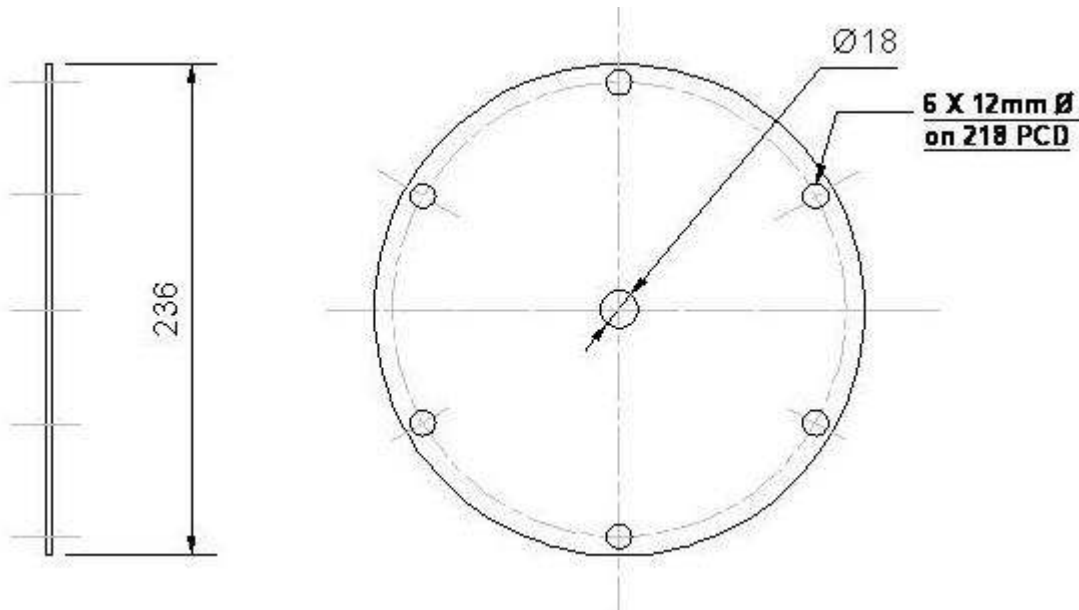


**Figure 5:** Depulping chamber face plate

A number of spikes consisting of 6.35mm rods of length 165mm are welded unto flat bars attached to a hub to agitate the contents of the

separation chamber and encourage separation of the seeds from the pulp. This is illustrated in figure 6.

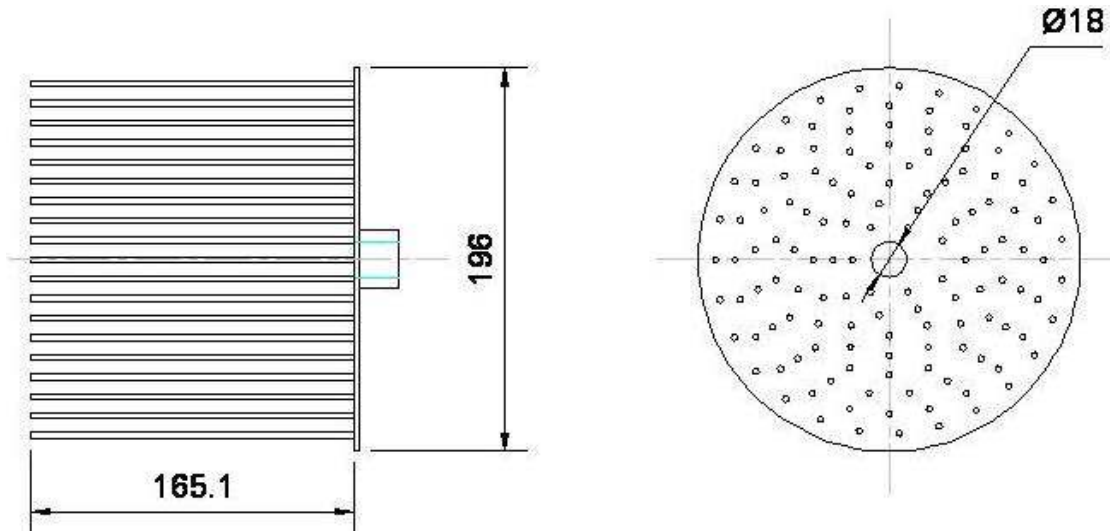
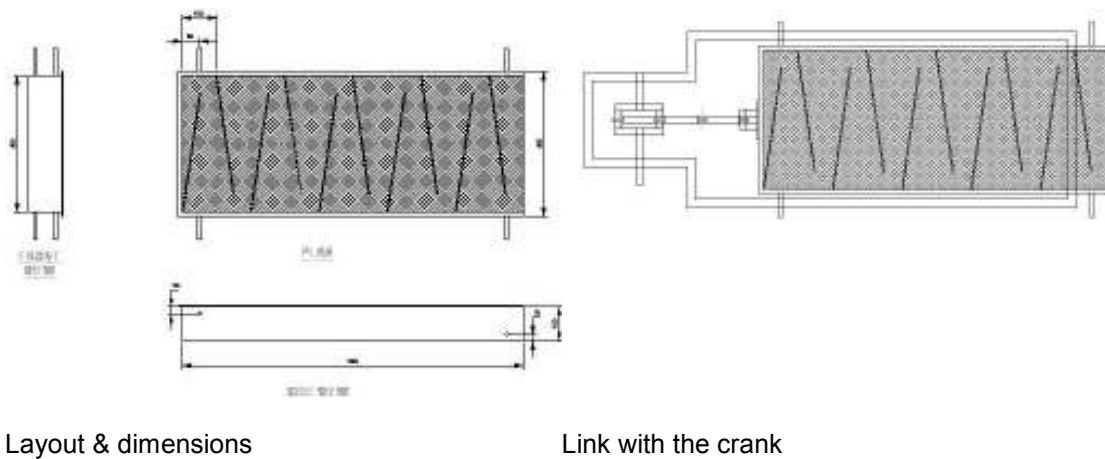


**Figure 6:** Conceptual arrangement of spikes in the depulping chamber

The washed seeds are separated in the separation chamber. This is essentially a rectangular tank with horizontal baffles to slow down the flow of slurry. The underside of the chamber is fitted with a perforated tray, while the

top of the chamber is covered with a water tank. The length and width of the tray are 1000mm and 400mm respectively, with a total of 10 baffles introduced, as shown in figure 7.



Layout & dimensions

Link with the crank

**Figure 7:** Separator tray showing the arrangement of baffles and link with the crank

In this way, the mean effective length of the passage is almost 4m as calculated from the expression

$$L_p = 9.5[B^2 + (L/n)^2]^{1/2} \tag{1}$$

where,  $L_p$  = mean effective length of passage, B = width of tray = 400mm, L = length of tray = 1000mm, and n = no. of baffles =10. In this way, a complete separation of the seeds from the marshed pulp is ensured. The latter escape the chamber through the sieve. The separation chamber sieve itself consists of a metal gauge with rhombic openings whose maximum axial

dimensions are less than those of the seeds. This is available commercially with the trade name "vent net".

The baffles consist of gauge 20 galvanized steel sheet of dimension  $360 \times 75$  mm, inclined at  $14^\circ$  (as shown in figure 8). The material is chosen for low weight and corrosion resistance.



**Figure 8:** Separator tray with baffles inclined at  $14^\circ$  to the tray axis

The separation chamber is covered with a six-litre capacity steel water tank dimensioned to fit the rim of the chamber tray, namely:  $1000 \times 400 \times 15$  mm. The base of the tank has

perforations to allow for the exit of water jets. Gauge 22 galvanized steel sheet is selected for the cover plate. Top and bottom views of the tank after construction are shown in figure 9.



Top View



Bottom View

**Figure 9:** Water tank doubling as separation chamber cover

### 2.3 Crank-Rocker System

For greater effectiveness, the separation chamber is agitated slowly through a crank-rocker mechanism described in Mabie & Ocvirk

(1965), Shigley & Mitchel (1997) and Norton (1999). The system consists of a crank (figure 10), a coupler (figure 11) and rockers.

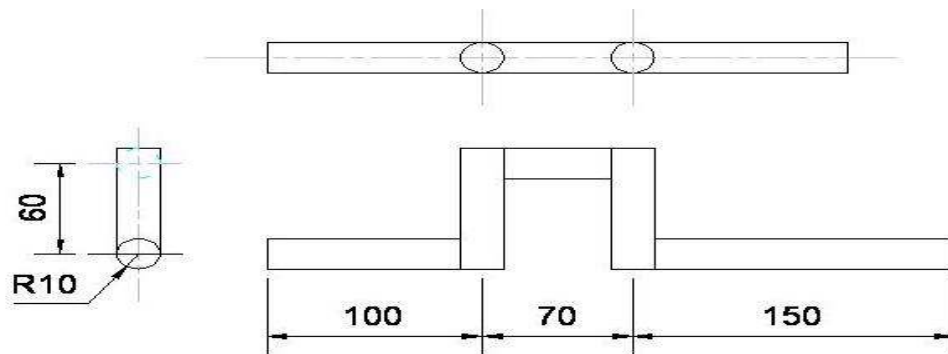


**Figure 10:** Schematic diagram of the crank

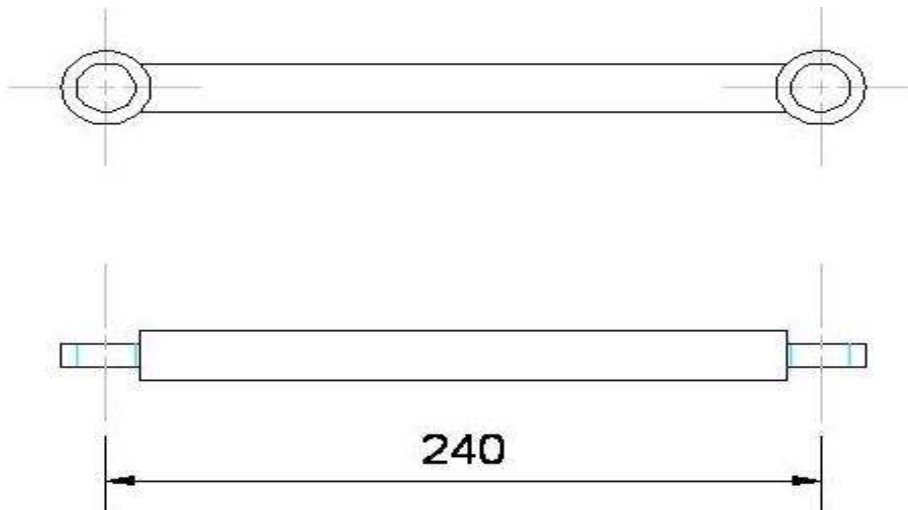


**Figure 11:** Schematic diagram of the coupler

The combination of crank, coupler, rockers and separation chamber resulting in the oscillating motion of the separation chamber can be analysed by representing the combination with a six bar, crank and double rocker mechanism, (isomer II of the so-called Watt's linkage described in Norton (1999) (see figure 12)). This

consists essentially of two four bar linkages in series and was analysed as such. To simplify the analysis, the system is decomposed into two four-bar linkage vector loops such that the solution of the first loop is used as input to the second loop.

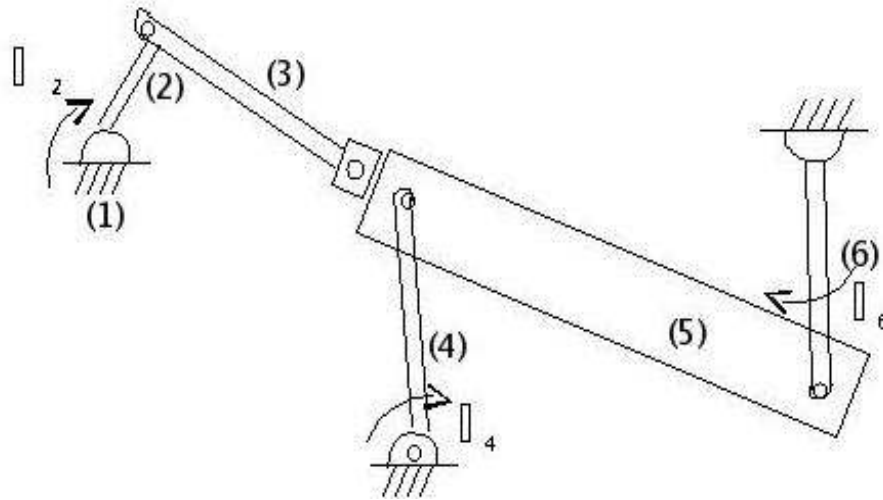


**Figure 12:** Schematic diagram of the crank-rocker mechanism

A computer program for the sequence, "SIXBAR" reported in Norton (1999) was used to analyze the system and obtain values of linear

and angular positions, velocities, accelerations and forces in the links in the system. The details are presented in Asiegbu (2004) and Njoku

(2004). The components were dimensioned as appropriate. To design the slider, the oscillation amplitude (stroke) of the separation tray was chosen to be 160 mm. This stroke length was to enable the seeds sweep through the baffle-to-baffle distance (100mm) with each oscillation. The crank radius was set equal to half of the separation chamber length; thus  $r \leq 160/2 = 80$  mm.

The coupler or connecting rod links the crank to the tray and consists of a rod welded at the two ends to journal bearings, which serve as joints to the crank and separation tray. According to Norton (1999), optimum crank to coupler ratio,  $r/l$  should lie between 1/3 and 1/5;  $r/l = 1/3$  was chosen, based on overall machine dimension considerations. Thus length of coupler,  $l = 3r = 3 \times 80 = 240$  mm. Some

specifications of the coupler are shown in figure 11.

The connecting rod is hinged at one end to the frame of the machine through a rocker. The lengths of the rockers were chosen to be 400mm and holes spaced 15mm apart were drilled to allow for adjustment of their lengths.

#### 2.4 Kinematic Analysis

Kinematic analysis of the mechanism was undertaken to determine the position and velocity of key points on the crank-shaft-coupler system at any angular position of the driving link using the simplified six-bar linkage shown in figure 12.

A position analysis of this system will yield the following relations for the coupler position B, coupler angle  $\theta_3$  and rocker angle  $\theta_4$ .

$$B_x = \frac{(a^2 - b^2 + c^2 - d^2) - (2A_y B_y)}{2(Ax - d)} \quad (2)$$

$$B_y = \frac{-Q \pm (Q^2 - 4PR)^{0.5}}{2P} \quad (3)$$

where,

$$A_y = a \cos \theta_2 \quad (4)$$

$$A_y = a \sin \theta_3 \quad (5)$$

$$B_x = A_x + b \cos \theta_2 \quad (6)$$

$$B_y = A_y + b \sin \theta_3 \quad (7)$$

$$P = \left( \frac{A_y}{A_x - d} \right)^2 + 1 \quad (8)$$

$$Q = \frac{2 A_y (d - S)}{A_x - d} \quad (9)$$

$$R = (d - S)^2 - c^2 \quad (10)$$

$$S = \frac{a^2 - b^2 + c^2 - d^2}{2(A_x - d)} \quad (11)$$

$$\theta_3 = \tan^{-1} \frac{B_y - A_y}{B_x - A_x} \quad (12)$$

$$\theta_4 = \tan^{-1} \frac{B_y}{B_x - d} \quad (13)$$

Using the computer program "SIXBAR" reported in Norton (1999), the variations of linear and angular positions,  $B_x, B_y, \theta_3$  and  $\theta_4$  with  $0 < \theta_2 < 360$  were determined. The angular positions are plotted in figure 13.

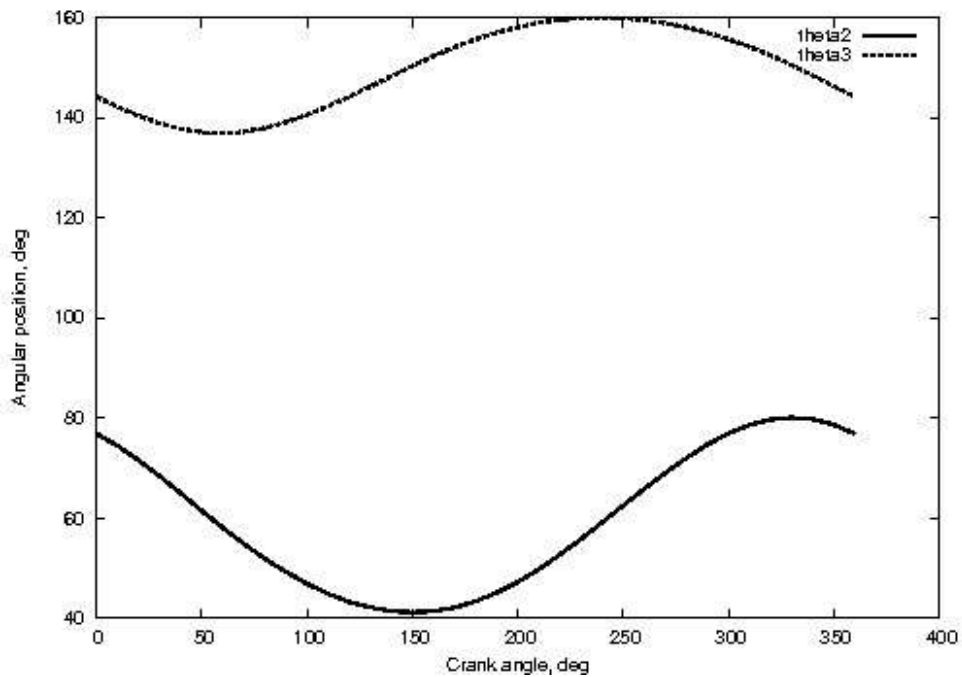


**Figure 13:** Angular positions of elements of the crank-rocker mechanism for various crank angles

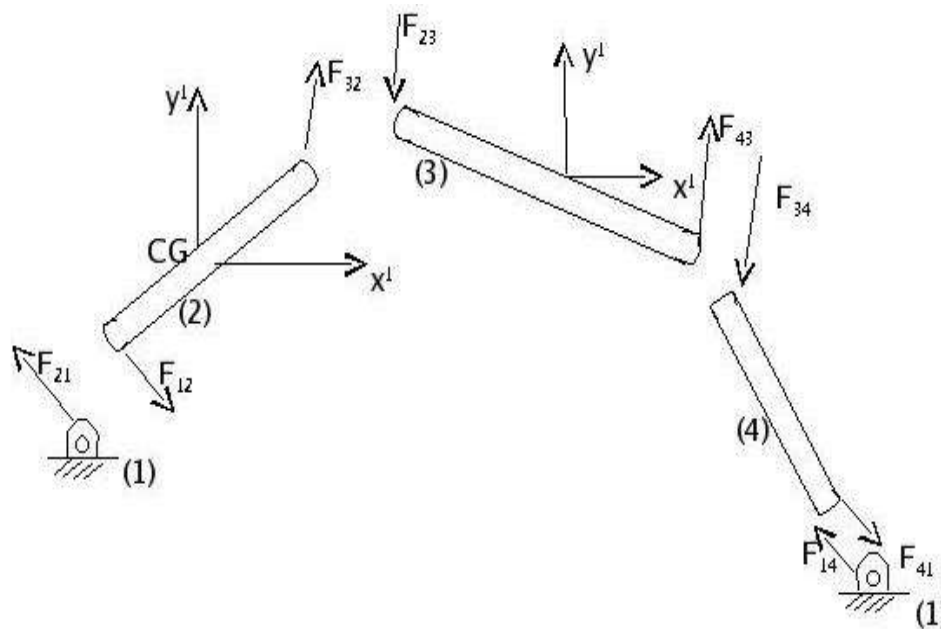


**Figure 14:** Parameters for the dynamic force analysis

Parameters for the velocity analysis of a four bar mechanism are as shown in figure 14.

The velocity analysis of the system yields appropriate relations for angular velocities of

coupler and rockers,  $\theta_3$  and  $\theta_4$  respectively, the absolute velocities of points A and B,  $V_A$  and  $V_B$  respectively and the relative velocity  $V_{BA}$ , for an input crank angular velocity  $\theta_2$  :

$$\omega_3 = a \frac{\omega_2 \sin(\theta_4 - \theta_2)}{b \sin(\theta_3 - \theta_4)} \quad (14)$$

$$\omega_4 = \omega_2 \frac{a \sin(\theta_2 - \theta_3)}{b \sin(\theta_4 - \theta_3)} \quad (15)$$

$$V_a = a \omega_2 \quad (16)$$

$$V_B = c \omega_4 \quad (17)$$

$$V_{BA} = b \omega_3 \quad (18)$$

As a design decision, a speed of 150 oscillations per minute was selected for the separation tray; this translates to a speed of 150 revolutions per minute for the crank. Thus,

$$\omega_2 = \frac{2\pi N_2}{60} = 15.71 \text{ rad/sec} \quad (19)$$

A chart of variations of  $\omega_3$ ,  $\omega_4$ ,  $V_a$  and  $V_B$  with  $0 < \theta_2 < 360$  were obtained using the program "SIXBAR". The results are plotted in figure 15.

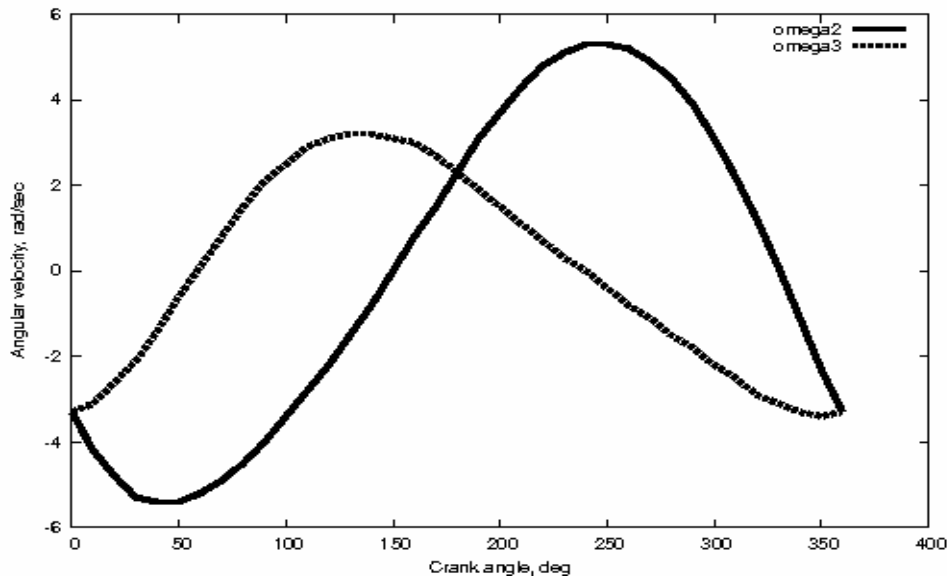


**Figure 15:** Angular velocity of elements of the crank-rocker mechanism for various crank angles

### 2.5 Dynamic Analysis

In order to specify the material and physical properties of the system as well as the physical shape of the crank-connecting-rod-rocker

system, a dynamic analysis of the forces acting at key points on the mechanism are determined. In turn, this requires an acceleration analysis, which is undertaken using the specifications in

figure 14.

An acceleration analysis of this system yields relations for angular accelerations of coupler and rocker,  $\alpha_3$  and  $\alpha_4$  respectively, the normal and tangential accelerations  $A_A^N$ ,  $A_A^T$ ,

$A_B^N$  and  $A_B^T$ , respectively at points A and B, and the normal and tangential relative accelerations  $A_{BA}^N$  and  $A_{BA}^T$ , respectively for an input crank angular velocity  $\omega_2$ :

$$\alpha_3 = \frac{A \cos \theta_4 - B \sin \theta_4}{b(\sin \theta_4 \cos \theta_3 - \sin \theta_3 \cos \theta_4)} \quad (20)$$

$$\alpha_4 = \frac{A \cos \theta_3 B \sin \theta_3}{c(\sin \theta_4 \cos \theta_3 - \sin \theta_3 \cos \theta_4)} \quad (21)$$

where,

$$A = a\alpha_2 \sin \theta_2 + a\omega_2^2 \cos \theta_2 + b\omega_3^2 \cos \theta_3 - c\omega_4^2 \cos \theta_4 \quad (22)$$

$$B = a\alpha_2 \cos \theta_2 - a\omega_2^2 \sin \theta_2 - b\omega_3^2 \sin \theta_3 + c\omega_4^2 \sin \theta_4 \quad (23)$$

$$A_A^T = a\alpha_2 \quad (24)$$

$$A_A^N = -a\omega_2^2 \quad (25)$$

$$A_{BA}^T = b\alpha_3 \quad (26)$$

$$A_{BA}^N = -b\omega_3^2 \quad (27)$$

$$A_B^T = c\alpha_4 \quad (28)$$

$$A_B^N = -c\omega_4^2 \quad (29)$$

Computed results for  $\alpha_3$  and  $\alpha_4$  for the range  $0 \leq \theta_2 \leq 360$  are plotted in figure 16.

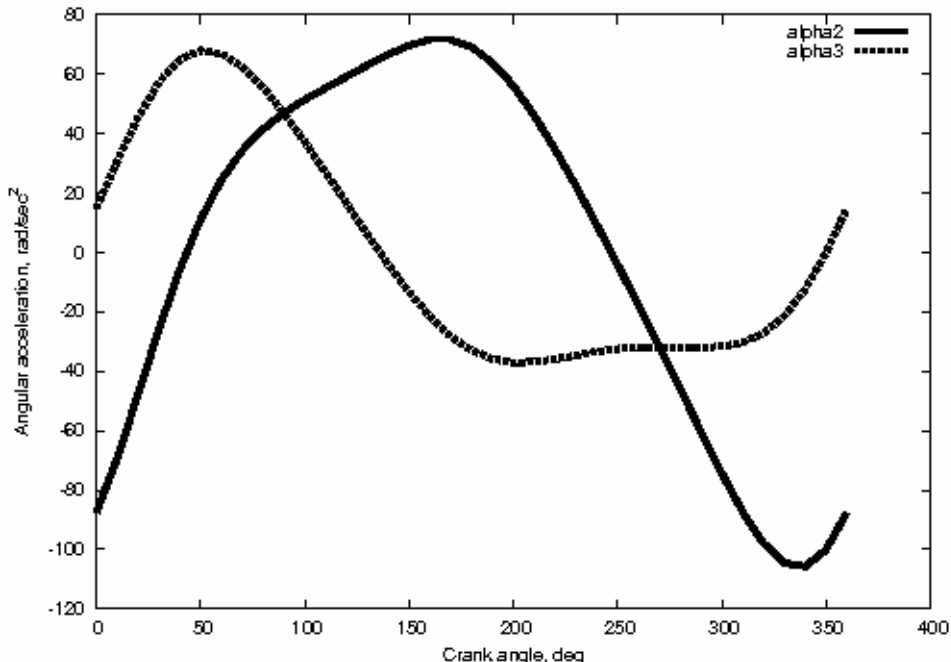


Figure 16: Angular acceleration of crank-rocker elements as a function of crank angle

**2.5.1 Dynamic Force Analysis**

Parameters for the dynamic force analysis of the four bar mechanism are as shown in figure 14.

This analysis yields the  $9 \times 9$

system of equations shown in table (1). The solutions give forces on all components and the torque on the crank for any specified crank position  $\theta_2$  and angular velocity  $\omega_2$

**Table 1:** Matrix of force components

1	0	1	0	0	0	0	0	0	$F_{12x}$	$m_2 a_{G2}$
0	1	0	1	0	0	0	0	0	$F_{12y}$	$m_2 a_{G2}$
$-R_{12y}$	$R_{12x}$	$-R_{32x}$	0	0	0	0	0	1	$F_{32x}$	$I_{G2} \alpha_2$
0	0	-1	0	1	0	0	0	0	$F_{32y}$	$m_3 \alpha_{G3}$
0	0	0	-1	0	1	0	0	0	$F_{43x}$	$m_3 \alpha_{G3}$
0	0	$R_{23y}$	$-R_{23x}$	$-R_{43y}$	$R_{43x}$	0	0	0	$F_{43y}$	$I_{G3} \alpha_3$
0	0	0	0	-1	0	1	0	0	$F_{14x}$	$m_4 \alpha_{G4}$
0	0	0	0	0	-1	0	1	0	$F_{14y}$	$m_4 \alpha_{G4}$
0	0	0	0	$R_{34y}$	$-R_{34x}$	$-R_{14y}$	$R_{14x}$	0	$T_{12}$	$I_{G4} \alpha_4$

Employing flat mild steel bars of number  $n$ , thickness  $t$ , width  $b$  and length  $l$ , the mass of each member is computed from the expression  $m = \rho l b t$ . Assuming that the

centres of gravity, CG's of each link is located at the geometric centre, the mass moment of inertia is given by

$$I_G = \frac{m(b^2 + L^2)}{12} \tag{30}$$

The computed values of  $m$  and  $I_G$  for each link are given in table 2.

**Table 2:** Dimensions and other dynamical parameters of links in the six-bar linkage

Link	Length, L (mm)	width, b (mm)	thickness, t (mm)	number of steel bars -	mass, m (kg)	moment of inertia, IG (kg m <sup>2</sup> )	Angle, $\theta$ (deg)	maximum force, $F_{ij}$ (N)	Maximum stress, $\sigma$ (MPa)
Crank	80	40	8	2	0.4	$2.67 \times 10^{-5}$	50	33.7	0.053
Coupler	240	20	6	1	0.225	$10.88 \times 10^{-5}$	50	29.8	0.248
Rocker (4)	400	20	6	3	1.123	$150.1 \times 10^{-5}$	60	34.6	0.144
Rocker (6)	400	20	6				60	93.9	0.047

The force components  $F_{ij}$  given by equation (1) are described in the nomenclature section. The values of the forces on the links as well as the torque  $T_{12}$  within the range  $0 \leq \theta_2 \leq 360$  were obtained using the program

"SIXBAR". The x- and y-components of each force, the magnitude and its angular position were also determined. Typical values for the frame and crank are shown in figure 17. Further details are reported in Enibe (2005).

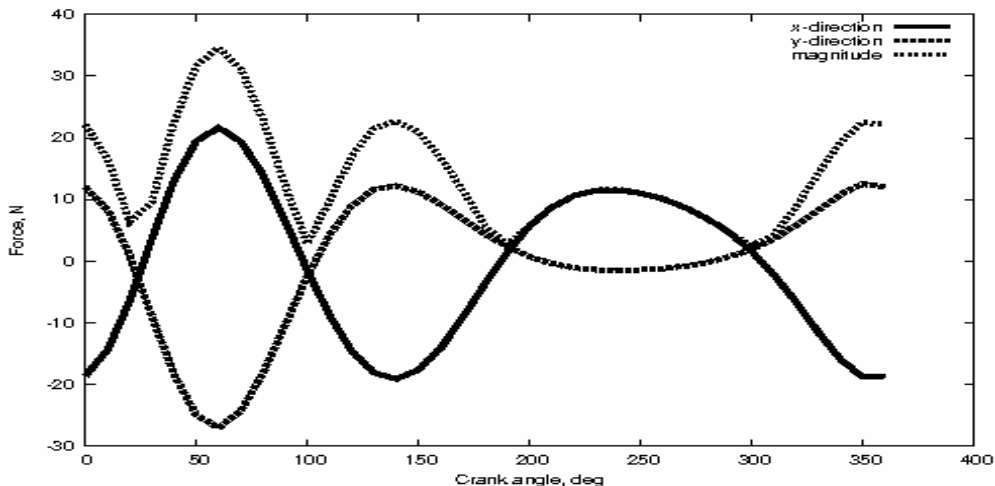


**Figure 17:** Components of the force between frame and rocker,  $F_{14}$

### 2.6 Dynamic Stress Analysis

From the detailed force analysis presented previously, the maximum axial force on each link and its direction were obtained. The maximum stress is then given by  $\sigma_j = F_{ij, mag} / A_j$ . Values of  $F_{ij, mag}$ ,  $\theta$  and  $\sigma$  are shown in table 2. It can be seen that these stresses are less than the material yield stress  $\sigma_y = 450$  MPa. It was observed that the torques, forces and accelerations decrease with decreasing angular

velocity of crank. The values of the forces at other rotational speeds were also computed (see Asiegbu (2004) and Njoku (2004)).

### 2.7 Flywheel

The fluctuating torque requirement of the crank, which results from the reciprocating motion of the mechanism, necessitates the use of a flywheel. The mass moment of inertia of the required flywheel  $I_s$ , is obtained from the equation

$$E = 0.5 I_s (\omega_{max}^2 - \omega_{min}^2) \quad (31)$$

Expanding, this becomes

$$E = 0.5 I_s (\omega_{max} + \omega_{min})(\omega_{max} - \omega_{min})$$

Hence, we obtain

$$E = 0.5 \frac{I_s \times 2 \times (\omega_{max} + \omega_{min})}{2} \omega_{avg} \frac{(\omega_{max} - \omega_{min})}{\omega_{avg}}$$

We note that the coefficient of fluctuation,  $k$ , is defined by

$$\frac{\omega_{max} - \omega_{min}}{\omega_{avg}} = k = \text{coefficient of fluctuation} \quad (32)$$

Thus, the energy of the flywheel, E, is then given by

$$E = I_s \omega_{avg} \omega_{avg} k = I_s \omega_{avg}^2 k \quad (33)$$

Hence, the mass moment of inertia is given by

$$I_s = \frac{E}{\omega_{avg}^2 k} \quad (34)$$

The energy of the flywheel, E is obtained from the tabulated data by numerical integration using the trapezoidal rule, hence

$$E = \int_{\theta_{at\omega_{min}}}^{\theta_{at\omega_{max}}} (T_L - T_{avg}) d\theta \quad (35)$$

Substituting, we have  $E = -0.9 - (-0.9) = -1.8$  Nm

Choosing  $k = 0.05$ , we have  $I_s = 0.1457 \text{ Nm}^2 \equiv mr^2$

### 2.8 Motor Selection

Power requirement for the machine is based on the torque input needed to drive the reciprocating separation tray. This is given by

$$P = T_{max} \omega_2 \quad (36)$$

Where,  $T_{max}$  = maximum torque input to crank = 1Nm,  $\omega_2$  = angular velocity of crank = 15.77rad/s. Hence,  $P = 1 \times 15.77 = 15.77$  W. This implies that the power in horse power units is

$P_{hp} = 15.77 / 746 = 0.021$  hp. Based on this, a 0.5 hp motor was selected, with a speed of 1425 revolutions per minute.

## 2.9 Pulleys

The angular velocity of the de-pulper pulley,  $\omega_d$  may now be determined. Results of tests reported in Enibe (2001) showed that for the batch processor, the angular speed at which the fruit was safely processed without damage to the seeds was 137rpm = 14.35 rad/s. At this speed, the maximum kinetic energy of impact with which the agitator strikes the seeds is given by

$$K E_a = 0.5 m_s V_a^2 = 0.5 m_s \omega_a^2 r_a^2 = 0.5 \rho_s V_s \omega_a^2 r_a^2 \quad (37)$$

Where,  $\omega_a$  = angular velocity of agitator = 14.35 rad/s,  $r_a$  = length of agitator = 190.5mm,  $V_s = 0.75\pi r^3 = 0.75(3.705 \times 10^{-3})^3 = 2.13 \times 10^{-7} m^3$  Hence,

$K.E_a = 0.5 \times 928 \times 2.13 \times 10^{-7} \times 14.35^2 \times (10.5 \times 10^{-3})^2 = 7.39 \times 10^{-4}$  J. This was taken to be an acceptable kinetic energy of impact with which de-pulping action will be achieved without damage to the seeds. This K.E was selected as that to which  $K.E_d$ , the K.E of impact of the spikes on the seeds will be limited. Thus,

$$K.E_d = K.E_a = 0.5 \rho_s V_s \omega_d^2 r_d^2 \quad (38)$$

where,  $r_d$  = radius of the flat bars onto which the spikes are welded. Thus, we have

$$\omega_d = \left( \frac{2K.E_d}{\rho_s V_s r_d^2} \right)^{0.5} \quad (39)$$

Substituting, we have  $\omega_d = 27.9$  rad/s. Also,  $N_d = 60\omega_d / (2\pi) = 266.45$  rpm.

Ratio of diameters of depulper pulley to motor pulley is given by:

$$d_d = \frac{N_m}{N_d} \equiv \frac{\omega_m}{\omega_d} \quad (40)$$

where the subscripts  $d$  and  $m$  refer to de-pulper and motor, respectively. Thus,

$$d_d = \frac{N_m d_m}{N_d} = \frac{1425 d_m}{266.45} = 171.2 \text{ mm} \quad (41)$$

## 2.10 Separator/Crank Shaft

As indicated earlier, a speed of 150rpm was chosen for the separator pulley. Letting the subscript  $s$  refers to the separator pulley, we have

$$\frac{d_s}{d_m} = \frac{N_m}{N_s} = \frac{d_m \times N_m}{N_s} \quad (42)$$

Substituting, we have  $d_s = 304$  mm since  $d_m = 9.5 \times 32$  mm .

**2.11 De-pulper Shaft**

The critical load on this shaft is due to the tension in the belts on the de-pulper pulley. The shaft layout is as shown in figure 18.

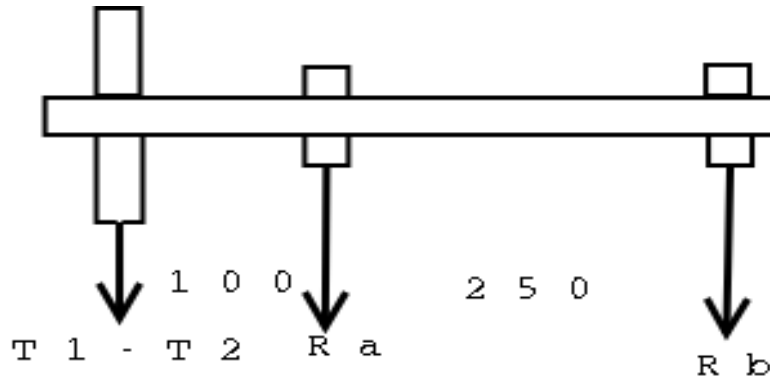


**Figure 18:** De-pulper shaft layout

The power rating of the pulley is given by

$$P_m = (T_1 - T_2)V_p = (T_1 - T_2)\omega_p r_p \tag{43}$$

where,  $(T_1 - T_2)$  = resultant tension in the belts, which is identical to the axial force on shaft by pulley. Now,  $\omega_d = 27.9$  rad/s. Selecting a pulley diameter  $d_d = 170$  mm, then  $r_d = 85\text{ mm} = 0.085$  m. Thus,  $T_1 - T_2 = P_m / (\omega_d r_d) = 0.5 \times 746 / (27.9 \times 0.085) = 157.28\text{ N}$ . Taking moments about A, in the direction perpendicular to belt tensions,  $(T_1 - T_2) \times 100 = R_b \times 250$ , yielding  $R_b = (T_1 - T_2) \times 100 / 250 = 157.28 \times 0.4$ , hence  $R_b = 62.91$  N. For static equilibrium of the shaft, the condition that  $\sum F_y = 0$ , must be satisfied. Thus,  $(T_1 - T_2) - R_A + R_b = 0$ . Substituting for  $R_b$  and  $T_1 - T_2$ , we have  $R_A = 220.19$  N. Bending moment at A is given by  $M_A = (T_1 - T_2) \times 0.100 = 157.28 \times 0.100 = 15.73$  Nm. Torque on the shaft is given by  $M_t = (T_1 - T_2) \times d_p = 157.28 \times 0.170 = 26.74$  Nm. The shear force and bending moment diagrams in the plane of belt tension direction are shown in figure 19.

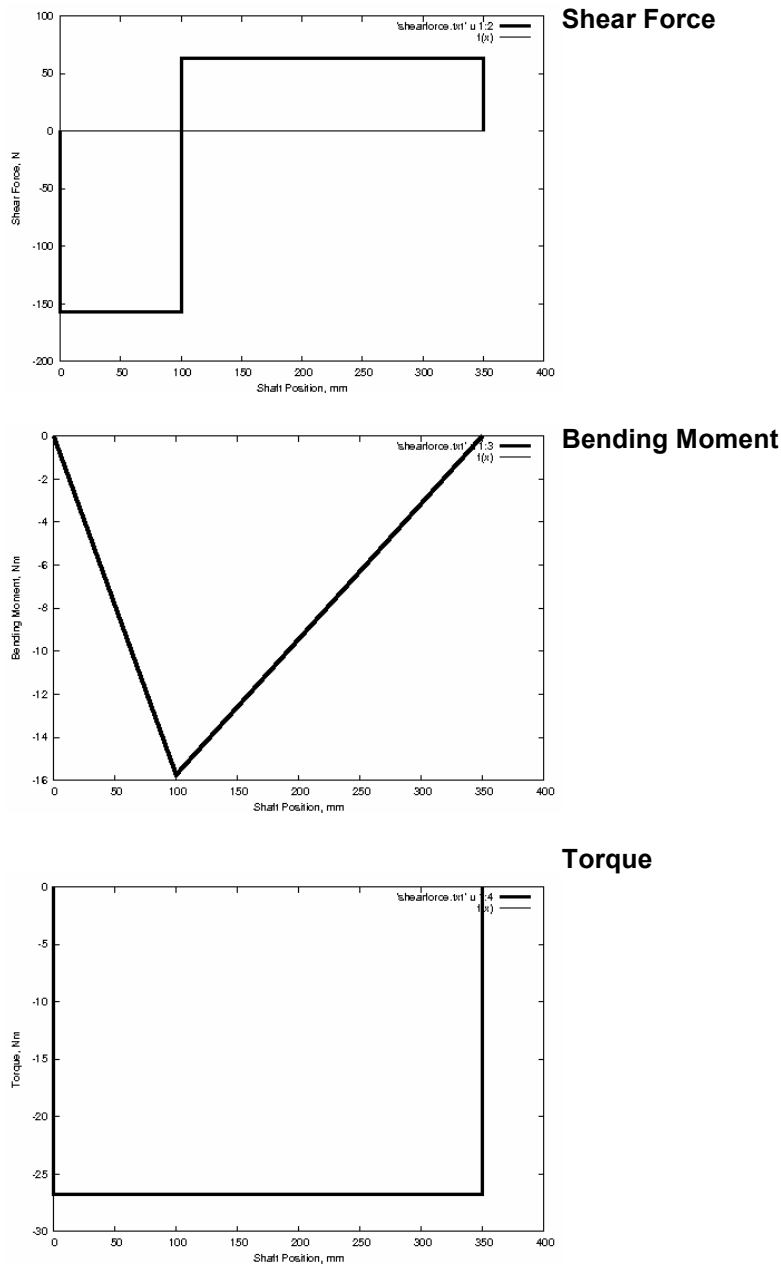


**Figure 19:** Shear force, bending moment and torque diagrams of de-pulper shaft

The critical load on the shaft is at the bearing point A, and on the basis of cost and availability, cold drawn AISI 1020 steel having  $S_{ut} = 530$  MPa and  $S_y = 450$  MPa, machined, is selected as shaft material. Design calculations are based on a factor of safety,  $n =$

3.0, for dynamic loading. From the literature, for  $S_{ut} = 530$  MPa, while the endurance limit,  $S'_e \approx 215$  MPa. According to Bhandari (1999), the endurance strength of the shaft  $S_e$  is related to its endurance limit,  $S'_e$  by the expression

$$S_e = k_a k_b k_c k_d S'_e \tag{44}$$

where the design factors  $k_a$  to  $k_d$  are specified in the nomenclature section. Substituting, this yields  $S_e = 130.68$  MPa. Using the Soderberg equation, the diameter of the shaft,  $d$  is given by

$$d = \left\{ \frac{32n}{\pi} \left[ \left( \frac{M_t}{S_y} \right)^2 + \left( \frac{M_B}{S_e} \right)^2 \right]^{0.5} \right\}^{0.5} \quad (45)$$

At the critical point,  $M_t = 26.74$  Nm,  $M_B = 15.73$  Nm, thus  $d = 0.016$  m.

A shaft size of 20mm was selected because of availability of material and bearings of appropriate size.

### 2.12 Flexible Connector

A flexible connector conveys de-pulped fruit slurry from the de-pulping chamber to the separation chamber. Vulcanized rubber tubing was selected for this.

## 3. CONSTRUCTION

### 3.1 Hopper

To construct the hopper, 20 gauge galvanized steel was cut into the shape of the development of the frustum of a cone, and rolled mechanically to form the hopper's shape and joined at the ends. A photograph of the unit integrated with the depulping chamber is shown in figure 20.



Figure 20: Photograph of the hopper and depulping chamber

### 3.2 De-pulping chamber

In the case of the depulping chamber, 20 gauge galvanized steel was cut into a rectangular shape and rolled mechanically into a cylinder to form the housing. It was joined at the edges. A flange was formed mechanically at one end and the other end was closed with a circular disk of the same

material. A circular disk was also cut to form the chamber cover plate. The cover plate is attached to the housing using size M10 nuts and bolts, which pass through holes, drilled in the flange of the housing and in the cover plate. The hopper and an outlet were welded to openings cut into the de-pulping chamber housing at its top and

bottom, respectively.

### 3.3 Separation Chamber

The separation chamber tray was also fabricated from gauge 20 galvanized steel sheets. It was formed into the desired shape mechanically and covered beneath with a metal mesh. Baffles were welded to the inner sides of the tray and attached to the metal mesh base using copper wires. A water spray tank cover was fabricated from gauge 22 galvanized steel sheets. Holes were punched into the base to create outlets for jets of water. A plastic back-nut was screwed to the top of the tank to create an inlet for water. Holes were drilled into the sides of the tray using a hand drill to allow for the attachment of the

rockers by means of M12 bolts and nuts. An inside view of the separation chamber is shown in figure 8, while top and bottom views of the water tank constituting the cover are shown in figure 9. The baffles may be clearly seen inclined at an angle to the tray axis.

### 3.4 Rockers

The rockers were formed from mild steel flat bars cut to size and welded to form the proper shape, to make for rigidity and to prevent the swaying of the tray sideways.

Holes were drilled into the main rocker bars, spaced at 15mm to allow for adjustment of the length of the rockers. A photograph of the system in-situ is shown in figure 21.



**Figure 21:** Photograph of the Crank-Rocker Mechanism for agitating the separation chamber

### 3.5 Frame, Shaft, Crank and Coupler

The frame was constructed using 2-inch angle bars, cut to size and welded together. The overall dimension of the frame was 1555×430×540 mm. The shafts were machined to size (20mm) on a lathe machine, and mounted on bearings attached to the frame by means of screws and bolts (see figure 18).

The crank was cut from an 8mm thick flat bar. Holes of 20mm diameter were drilled into the ends of the crank bars so cut, and the crankshaft inserted into the holes in the crank bars. The crank bars were then welded to the shaft. The other ends of the crank bars were connected by means of M17 nuts and bolts.

The coupler was cut from a 6mm thick

flat bar. Short lengths of hollow pipe were welded to the ends of the bar to form journal-bearing connectors to the crank and the separation tray, respectively.

### 3.6 Motor Sitting

The sitting for the motor was formed from 50.8mm (2-inch) angle bars. Slots were cut into the top of the sitting to make for adjustments of the motor in the transverse direction, by means of M19 nuts and bolts the sitting was attached to the

frame through slots in the frame to make for adjustments of the sitting in the vertical direction.

### 3.7 Material Specifications

A breakdown of the material and cost details for the construction of the machine is shown in table 3. All of the materials were purchased from shops within Enugu and Anambra States of Nigeria. Only some of the direct cost items have been included.

**Table 3:** Material and cost specifications

S/No	DESCRIPTION	SPECIFICATIO NS	QTY	UNIT COST (N= )	COST (N= )
01	Galvanized Steel Sheet	Gauge 20	1	1500	1500
		Gauge 22	1	1200	1200
02	Shafts	20" x 1" dia.	2	200	400
03	Pillow bearings	P204	4	450	1800
04	Angle bars	2"	2	1600	3200
		1"	1	780	780
05	Pulleys	2 grove (32mm)	1	400	400
		Single grove (1ft)	1	900	900
06	Wire mesh	10mm x 5mm	Many	-	1200
07	Nuts, bolts & washers	M10 11 M12 8 M17 2 M19 12		-	400
08	Hub		1	400	400
09	Flat bars	6mm x 20mm	4	-	250
10	Tank back-nut	8mm x 40mm	1		
		Plastic	1	250	250
11	V-belts	A-56	1	150	150
		A-57	1	150	150
12	Vulcanized rubber tube		1	120	120

13	Stainless steel clip		1	50	50
14	Enamel paint	Ash colour	1 tin	120	120
15	Paint brush	-	1	40	40
16	1/4" rods	-	4	90	360
17	Electrodes		Many	-	180
18	Saw blades	-	2	120	240
19	Drillings	-	Many	-	230
20	Slots	-	Many	-	170
21	Labour	Tinker	Many	-	2500
		Welders	Many	-	3100
22	Transportation	-	Many	-	2580
23	Miscellaneous	-	Many	-	2345
	TOTAL				25,015

#### 4. EVALUATION

Two heads of breadfruit were left to ferment for some days, one partially and the other more completely. The breadfruit were sliced to appropriate sizes, measured and fed into the hopper.

##### 4.1 Testing

As a preliminary evaluation of the machine performance, the effect of the level of fermentation and the method of feeding were investigated for the de-pulping chamber only and for a shaft speed of 316.7 rpm.

In order to determine the effectiveness of the de-pulping chamber, 2042 cm<sup>3</sup> (2 litres) of well fermented fruit was introduced into the hopper, the machine was started and water supplied. The machine was kept running until all the fruit introduced had passed through the de-pulping chamber and collected at the chamber outlet. The machine was turned off. The quantity of water consumed as well as the time taken to complete the operation was determined.

The seeds in the slurry collected at the

outlet were sorted to obtain the number of seed completely de-pulped,  $N_1$ , the number of seeds partially de-pulped,  $N_2$  and the number of broken seeds,  $N_3$ . Fractions of completely de-pulped seeds  $N_1/N_0$ , partially de-pulped seeds  $N_2/N_0$ , and broken seeds  $N_3/N_0$ , were computed and expressed as percentages. The effectiveness was given by the first expression  $N_1/N_0$  and the ineffectiveness by [100 - effectiveness]. We note that the total number of seeds collected,  $N_0 = N_1 + N_2 + N_3$ .

This procedure was repeated with intermittent feeding of well fermented fruit, and then intermittent feeding of partially fermented fruit, for the same shaft speed.

##### 4.2 Results

The results of the tests are shown in table 4, from which the effect of the level of fermentation and method of feeding on the machine performance, shown in figure 22, is derived.

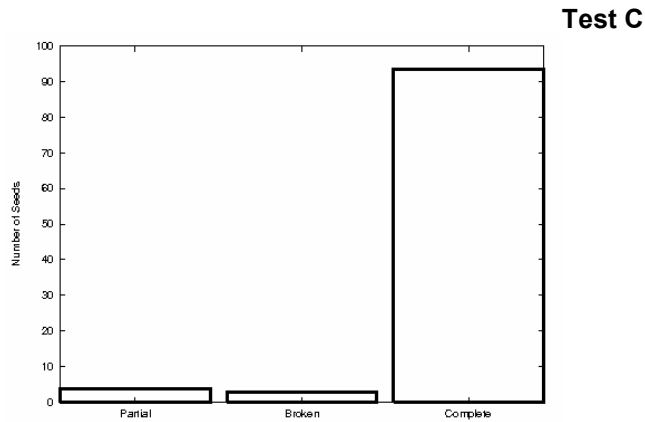
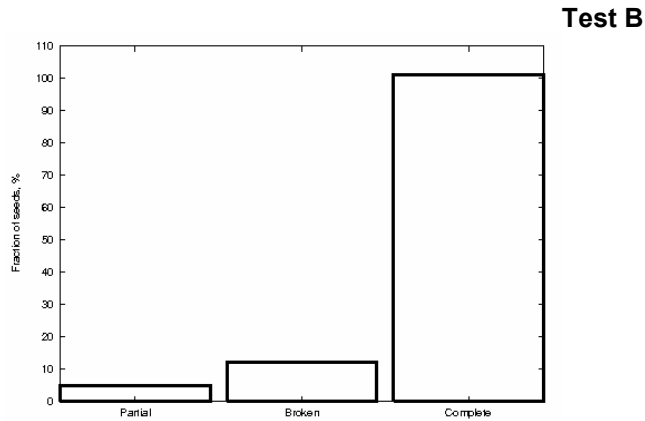
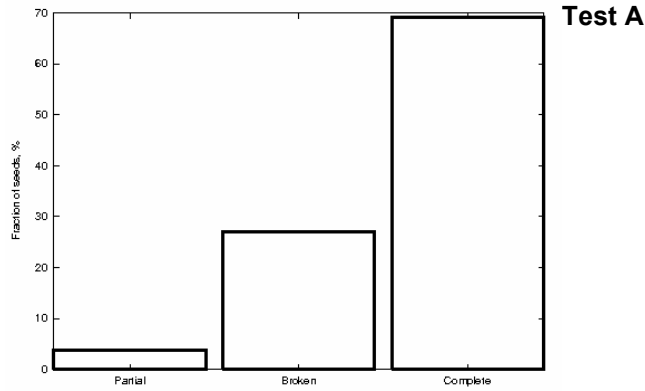


**Figure 22:** Effect of method of feeding and level of fermentation on machine performance  
 A = batch feeding of completely fermented fruit; B = intermittent feeding of completely fermented fruit; C = intermittent feeding of partially fermented fruit.

It may be seen that the effectiveness of the machine improved with intermittent feeding of the fruit into the machine as opposed to

choke/batch feeding. Also, the effectiveness improved when processing partially fermented fruit against well fermented fruit.

**Table 4:** Results of preliminary testing of machine de-pulping chamber

Sample	I	II	III
Vol. of fermented breadfruit used	2042 $cm^3$	1021 $cm^3$	1021 $cm^3$
Level of fermentation	Advanced	Advanced	Partial
De-pulping Shaft speed	316.7rpm	316.7rpm	316.7rpm
Total no of seeds recovered	52	118	242
No of seeds effectively de-pulped	36 69.2%	101 85.6%	226 93.4%
No of seeds incompletely de-pulped	2 3.8%	5 4.2%	9 3.7%
No of broken seeds	14 26.9%	12 10.2%	7 2.9%
Volume of water used	3 litres	1.5 litres	2 litres
Time taken (secs)	53	113 secs	110
Feed method	Batch	Intermittent	Intermittent

It was observed during the tests that the wire mesh fixed to the outlet of the de-pulping chamber for controlling the flow of the de-pulped fruit out of the chamber tended to prevent the flow of the slurry altogether, thus no conclusive deductions can be made of the times indicated as taken for the tests. The same also applies for the measured volume of water used up for the processes. Further work is continuing to evaluate the machine performance at various speeds and different conditions of the input material, as well as its acceptability by the stakeholders.

## 5. CONCLUSION

In conclusion, a feasible/practical mechanism has been conceived, designed, constructed and tested. With appropriate modifications and further improvement, this machine has the potential of

forming the basis for the industrial processing of the African breadfruit. It is hoped that this work will serve as a useful contribution towards realising the great potentials of this food crop as protein source and as a staple food. Further work is continuing to improve the machine performance and acceptability.

## ACKNOWLEDGMENTS

This work was supported under grant number 3 of 25/05/2002 via CBF/NET.FORM III of the African Forestry Research Network (AFORNET) of the African Academy of Sciences (AAS), Nairobi, Kenya. The authors are very grateful for the support.

The comments of anonymous reviewers are gratefully acknowledged.

## NOMENCLATURE

B	width, m
F	Force, N
$F_{12}$	Force of frame (1) on the crank (2) = - $F_{21}$
$F_{32}$	Force of coupler (3) on the crank (2) = - $F_{23}$
$F_{14}$	Force of frame (1) on rocker (4) = - $F_{41}$
$F_{54}$	Force of separation tray (5) on rocker (4) = - $F_{45}$
$F_{65}$	Force of rocker (6) on separation tray (5) = - $F_{56}$
$F_{16}$	Force of the frame (1) on the rocker (6) = - $F_{61}$
$F_s$	Unbalanced 'shaking force' on frame = $F_{21} + F_{41} + F_{61}$ , N
$k_a$	surface factor = 0.77 (for machined surface);
$k_b$	Size factor $\approx 0.88$ ;
$k_c$	Reliability factor = 0.897 (for 90% reliability) ;
$k_d$	Miscellaneous effect factor = 1 (due to generous factor of safety) .
L	length, m
m	mass, kg
r	radius, m
t	thickness, m
T	torque, NM
$T_{12}$	Torque input to crank, Nm
V	volume, $m^3$

## REFERENCES

- Asiegbu, C. P., 2004. "Design, construction and testing of a continuous-flow machine for the depulping and seed extraction African Breadfruit (*Treculia Africana*)", B. Eng. Project Report, Department of Mechanical Engineering, University of Nigeria, Nsukka, Nigeria.
- Bhandari, C. B., 1994. Design of Machine Elements. New Delhi: Tata McGraw-Hill.
- Enibe, S. O., 2001. Design, construction and testing of breadfruit depulping machine, Landwards, Summer 2001, 16–21.
- Enibe, S. O., 2005. Studies on the depulping of *treculia africana* (African breadfruit): Development of a continuous-flow depulping machine. Technical Report No. TARP/Depulping/2, African Forestry Research Network (AFORNET) of the African Academy of Sciences (AAS), Nairobi, Kenya.
- Iwe, M. O and Ngoddy, P. O., 2001. "Development of a mechanical dehulling process for the African breadfruit", Nigerian Food Journal, (19): 8–16.
- Mabie, H. H and Ocvirk, F. W., 1978. Mechanisms and Dynamics of Machinery. New York: John Wiley & Sons.
- Mbah, B. N., 2005. Propagation and early growth studies on *Treculia Africana*. In Enibe S. O., Mbah B. N., Akubuo C. O., Ani. J. O. and Enibe D. O. Propagation, Early Growth, Nutrition and Engineering Development Project on *Treculia Africana*, Scientific Report presented under grant number 3 of 25/05/2002 via CBFRR/NET.FORM III of the African Forestry Research Network (AFORNET) of the African Academy of Sciences (AAS), Nairobi, Kenya.
- Mott, L. C., 1976. Engineering Drawing and Construction. Oxford: Oxford

- University Press
- Njoku, H. O., 2004. "Design, construction and testing of a continuous-flow machine for the depulping and seed extraction African Breadfruit (*Treculia Africana*)", B. Eng. Project Report, Department of Mechanical Engineering, University of Nigeria, Nsukka, Nigeria.
- Norton, R. L., 1999. Design of Machinery: An introduction to the Synthesis and Analysis of Mechanisms and machines. New York: WCB/McGraw-Hill.
- Omobuwajo, T. O., Akande, E. A and Sanni, L. A., 1999. "Selected physical, mechanical and aerodynamic properties of African breadfruit (*Treculia africana*) seeds", Journal of Food Engineering, (40): 241–244.
- Omobuwajo, T. O., Ikegwuoha, H. C., Koya, O. A and Ige, M. T., 1999. "Design, construction and testing of a dehuller for African breadfruit (*Treculia africana*) seeds", Journal of Food Engineering, (42): 173–176.
- Orji, C. U., 2000. "Determination of some physical properties of breadfruit seeds (*Treculia africana*)", Conference Proceedings, 261–265.
- Shigely, J. E and Mitchell, L. D., 1997. Mechanical Engineering Design. New York: McGraw-Hill Book Company.
- Umoh, I. B. in Osagie, A. U and Eka, O. U., (Eds.) 1998. "Commonly used fruits in Nigeria", Nutritional Quality of Plant Foods. Benin: Post Harvest Research Institute of the University of Benin, 1998.